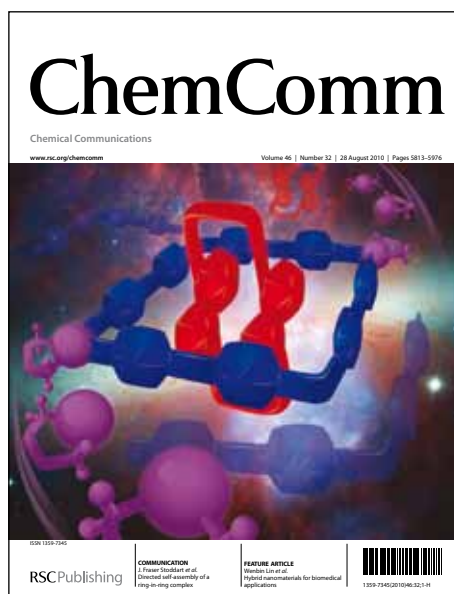


# ChemComm

## Accepted Manuscript



This is an *Accepted Manuscript*, which has been through the RSC Publishing peer review process and has been accepted for publication.

*Accepted Manuscripts* are published online shortly after acceptance, which is prior to technical editing, formatting and proof reading. This free service from RSC Publishing allows authors to make their results available to the community, in citable form, before publication of the edited article. This *Accepted Manuscript* will be replaced by the edited and formatted *Advance Article* as soon as this is available.

To cite this manuscript please use its permanent Digital Object Identifier (DOI®), which is identical for all formats of publication.

More information about *Accepted Manuscripts* can be found in the [Information for Authors](#).

Please note that technical editing may introduce minor changes to the text and/or graphics contained in the manuscript submitted by the author(s) which may alter content, and that the standard [Terms & Conditions](#) and the [ethical guidelines](#) that apply to the journal are still applicable. In no event shall the RSC be held responsible for any errors or omissions in these *Accepted Manuscript* manuscripts or any consequences arising from the use of any information contained in them.

Cite this: DOI: 10.1039/c0xx00000x

www.rsc.org/xxxxxx

ARTICLE TYPE

# Molecular luminogens based on restriction of intramolecular motions through host-guest inclusion for cell imaging

Guodong Liang,<sup>a,b,c</sup> Jacky W. Y. Lam,<sup>a,b</sup> Wei Qin,<sup>a,b</sup> Jie Li,<sup>a,b</sup> Ni Xie<sup>a,b</sup> and Ben Zhong Tang\*<sup>a,b,d</sup>

Received (in XXX, XXX) Xth XXXXXXXXXX 20XX, Accepted Xth XXXXXXXXXX 20XX

DOI: 10.1039/b000000x

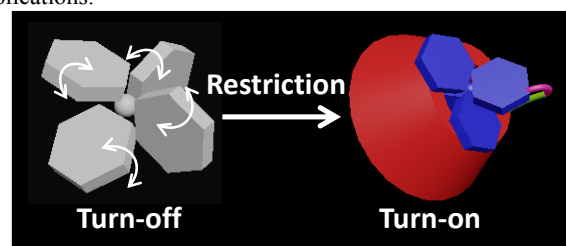
We developed a new strategy to restrict the motions of AIE molecules through host-guest inclusion, affording a catalogue of new molecular luminogens.

Luminogenic molecules with aggregation-induced emission (AIE) characteristics show strong light emission in the solid state and have attracted increasing interest recently due to their potential applications in biosensing, electroluminescence devices, cell imaging and so on.<sup>1</sup> Since our group reported the first AIE molecule in 2001,<sup>2</sup> a large number and a wide variety of AIE molecules have been synthesized based on the mechanism of restriction of intramolecular motions (RIM). Jiang and coworkers restricted the rotation of tetraphenylethene (TPE) by its confinement in intermolecular network, affording a catalogue of emissive conjugated microporous polymers.<sup>3</sup> Our group enhanced the emission efficiency of TPE in the solution state by locking its phenyl rings via covalent bond.<sup>4</sup> Dinca and coworkers immobilized functionalized TPE within rigid metal-organic framework through coordination polymerization, which turned its fluorescence on.<sup>5</sup> While chemical approaches are proved to be efficient to restrict the intramolecular motions, they involve variations in energy levels and molecular structures, both of which play important roles in the light emission process. This makes the effect of RIM process ambiguous and plausible. Thus, development of physical processes with minimal chemical

reactions to restrict the intramolecular motions is highly desirable.

Host-guest inclusion has attracted considerable attention in recent years for its wide applications in nano-machine, smart materials and so on.<sup>6</sup> The guest molecules are accommodated inside the cavity of host driven by physical interactions such as hydrophobic interaction, which offers a new opportunity for the preparation of new AIE luminogens. However, the utilization of host-guest inclusion to restrict the motions of AIE molecules is unprecedented to our best knowledge.

Herein, we report a new strategy for constructing single molecular luminogens through host-guest inclusion between cyclodextrins (CDs) and TPE. As a proof-of-concept demonstration, TPE functionalized with  $\alpha$ -,  $\beta$ - or  $\gamma$ -CD is selected as a model compound. We demonstrated that the phenyl rings of TPE resided in the cavity of CD, which restricted their motions and hence turned the fluorescence of non-emissive TPE on (Scheme 1). Since only physical interaction is involved, the effect of motion restriction on the light emission process can be identified. Moreover, given their high emission efficiency and good biocompatibility inherited from TPE and CD, the fluorescent inclusion complexes are promising for biological applications.



**Scheme 1** Schematic illustration of tetraphenylethene trapped inside the cavity of cyclodextrin

The CD-decorated tetraphenylethenes (TPE-CDs) were synthesized by esterification reaction of CD with monocarboxylic acid-substituted TPE (TPE-CO<sub>2</sub>H Scheme S1). Detailed procedures for the synthesis of TPE-CO<sub>2</sub>H and TPE-CDs were described in the Electronic Supporting Information (ESI). All the intermediates and desirable products were characterized by NMR and mass spectrometry and obtained satisfactory results corresponding to their molecular structures (Fig. S1–S11; ESI). The <sup>1</sup>H NMR spectrum of TPE- $\beta$ -CD as well

<sup>a</sup>HKUST-Shenzhen Research Institute, No. 9 Yuexing 1st RD, South Area, Hi-tech Park, Nanshan, Shenzhen, China 518057

<sup>b</sup>Department of Chemistry, Institute for Advanced Study, Division of Biomedical Engineering and Institute of Molecular Functional Materials, The Hong Kong University of Science and Technology, Clear Water Bay, Hong Kong, China

<sup>c</sup>DSAP lab, PCFM lab, School of Chemistry and Chemical Engineering, Sun Yat-Sen University, Guangzhou 510275, China

<sup>d</sup>Guangdong Innovative Research Team, SCUT-HKUST Joint Research Laboratory, State Key Laboratory of Luminescent Materials and Devices, South China University of Technology, Guangzhou 510640, China

†Electronic Supplementary Information (ESI) available: Materials and instruments, synthesis and characterization of the TPE-CDs, and NMR, mass, UV and CD spectra are supplied as Supporting Information. See DOI: 10.1039/b000000x/

as that of TPE-CO<sub>2</sub>H was shown in Fig. 1 as an example. A distinct signal attributed to the resonances of the phenyl protons adjacent to the ester group (a' in Fig. 1) was observed at  $\delta$  7.9. The absorptions of other protons (b', c' and d') at  $\delta$  7.1 and 6.9 were broad and weak, which was related to slow relaxation due to the restriction of their intramolecular motions.<sup>7</sup> Nuclear overhauser enhancement (NOE) cross-peaks between the TPE protons and the interior protons of CD cavity were observed in the 2D ROESY NMR spectrum of TPE- $\beta$ -CD, indicating that they were closely coupled.<sup>8</sup> This also suggested that most of the phenyl rings of TPE were immobilized in the CD cavity (Fig. S12). On the other hand, no NOE signals were detected between the resonance peak at  $\delta$  7.9 and those inside the  $\beta$ -CD cavity because they were far away from each other. Similar results were found in TPE- $\alpha$ -CD and TPE- $\gamma$ -CD (Fig. S13 and S14). From these results, the geometric structure of TPE- $\beta$ -CD and the optimized chemical structure of TPE were schematically illustrated in Scheme 2 and S2. While most of phenyl rings are restricted by cyclodextrin, still some of them are free for motions.

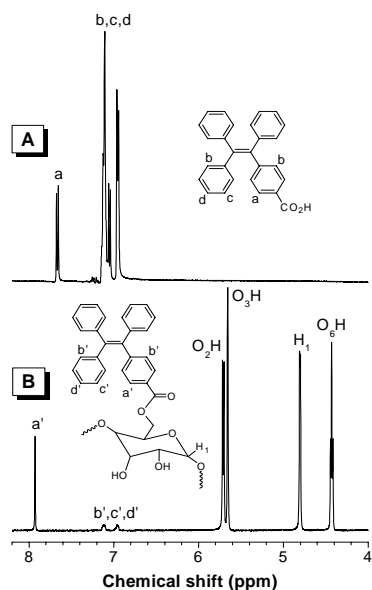
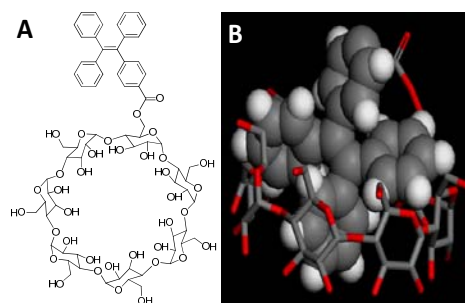


**Fig. 1** <sup>1</sup>H NMR spectra of (A) TPE-CO<sub>2</sub>H and (B) TPE- $\beta$ -CD in DMSO-*d*<sub>6</sub>.

The <sup>1</sup>H NMR signals of TPE- $\beta$ -CD were concentration-dependent. The peaks at  $\delta$  7.1 and 6.9 disappeared in high concentrated solution (Fig. S15), which illustrated the formation of intermolecular complex. It has been well known that adamantane has strong and specific interaction with cyclodextrin.<sup>9</sup> Adamantane enters preferentially into the cavity of cyclodextrin to form inclusion complex as compared with phenyl derivatives. After mixing with adamantane, the absorption peaks at  $\delta$  7.1 and 6.9 were clearly intensified (Fig. S16) because part of the phenyl rings were driven out from the cavity of  $\beta$ -CD owing to the strong and specific interaction of adamantane with CD. This further confirmed the formation of intermolecular complex in high concentrated solution.

The effect of cavity size of the CD on the RIM process was then investigated. Similar to TPE- $\beta$ -CD, the dilute solution of TPE- $\alpha$ -CD exhibited two broad peaks at  $\delta$  7.1 and 6.9, which

disappeared in high concentrated solution (Fig. S17). On the contrary, these peaks were still observed in the concentrated solution of TPE- $\gamma$ -CD, demonstrating the less restriction of  $\gamma$ -CD on the mobility of TPE (Fig. S18). Taking the signal at  $\delta$  7.9 as a reference, TPE- $\alpha$ -CD and TPE- $\gamma$ -CD exhibited the weakest and strongest absorption peaks at  $\delta$  7.1 and 6.9, respectively. The smaller cavity of  $\alpha$ -CD restricted the motions of phenyl rings of TPE in a greater extent than  $\gamma$ -CD with a larger cavity size (Table S1), thus resulting in weak aromatic signals.



**Scheme 2** (A) Chemical structure and (B) schematic illustration of the geometric structure of TPE- $\beta$ -CD.

The UV spectra of all the TPE-CDs showed a broad absorption band at 314 nm, which was blue-shifted from that of TPE derivative (TPE-C2) carrying no CD substituent (Fig. S19). This indicated that the TPE unit of TPE-CDs adopted a more twisted conformation in order to fit into the cavity of CD driven by hydrophobic interaction between the two components. Such interaction was verified using circular dichroism (CD) spectroscopy. A positive signal appeared in the absorption region of TPE in the CD spectra of all the TPE-CDs, suggesting that the CD unit induced the TPE moiety to pack in a helical fashion (Fig. S20).<sup>10</sup>

The fluorescence (FL) behaviors of the TPE-CDs were shown in Fig. 2. The dilute dimethylsulfoxide (DMSO) solution of TPE emitted weakly at 470 nm due to the intramolecular motions of the phenyl rings, which had efficiently consumed the energy of the excited states through nonradiative relaxation channels. In a sharp contrast, TPE- $\beta$ -CD showed a stronger FL at 410 nm, which was 60 nm blue-shifted from that of unsubstituted TPE (Fig. S21). The enhanced fluorescence revealed that the motions of the phenyl rings of TPE- $\beta$ -CD were somewhat restricted stemmed from the formation of inclusion complex. The TPE unit included in the CD cavity possessed a more twisted conformation, thus resulting in blue-shift in fluorescence. Compared to TPE- $\alpha$ -CD, TPE- $\beta$ -CD showed a weaker FL at 410 nm but emitted stronger than TPE- $\gamma$ -CD. The physical mixtures of TPE and CDs (TPE/CDs) radiated weakly at 470 nm in DMSO solutions under the same experimental conditions. The quantum yields of the TPE-CDs and their physical mixtures were determined using quinine sulfate as a reference (Fig. 2B). Bare TPE showed a low quantum yield (0.5%) in DMSO. On the other hand, TPE- $\beta$ -CD exhibited a 20-fold higher value. The value was further enhanced by mixing with adamantane, presumably due to the further activation of the RIM process by the bulky size of adamantane. Among the TPE-CDs, TPE- $\alpha$ -CD exhibited the highest FL quantum yield because the smaller cavity of  $\alpha$ -CD restricted the motions of phenyl rings more efficiently than the larger-sized  $\gamma$ -

CD cavity. Since all the TPE/CD mixtures exhibited low quantum yields, it demonstrated that covalent bonding of TPE with cyclodextrin is crucial for the formation of inclusion complex. The melding of TPE and CD into one molecule had brought the two units close apart, making the inclusion of the phenyl rings to the cavity of CD more easily.

To further verify the mechanism for the emission enhancement, time-resolved fluorescence measurements were carried out. The emission of bare TPE decayed exponentially with a lifetime of 1.41 ns (Fig. S22 and Table S2). In contrast, the excited state of TPE- $\beta$ -CD relaxed mainly through a slow pathway with a lifetime of 8.23 ns. More interestingly, TPE- $\beta$ -CD showed much lower non-radiative decay rate constant ( $10.2 \times 10^7 \text{ s}^{-1}$ ) and by far higher radiative decay rate constant ( $1.94 \times 10^7 \text{ s}^{-1}$ ) as compared to bare TPE ( $70.6 \times 10^7 \text{ s}^{-1}$  and  $0.355 \times 10^7 \text{ s}^{-1}$ , respectively, for bare TPE). In bare TPE solution, the energy of the excited states was annihilated efficiently by active intramolecular motions, which led to high non-radiative decay rate and low radiative decay rate as well as significantly shortened lifetime. On the other hand, the motions of the TPE unit were restricted in TPE- $\beta$ -CD, which blocked the non-radiative relaxation pathway and populated excitons that underwent radiative decay. Consequently, this gave rise to much lower non-radiative decay rate and higher radiative decay rate as well as longer emission lifetime. The time-resolved FL spectrum of TPE- $\alpha$ -CD resembled TPE- $\beta$ -CD, while the lifetime of TPE- $\gamma$ -CD was short and comparable to bare TPE.

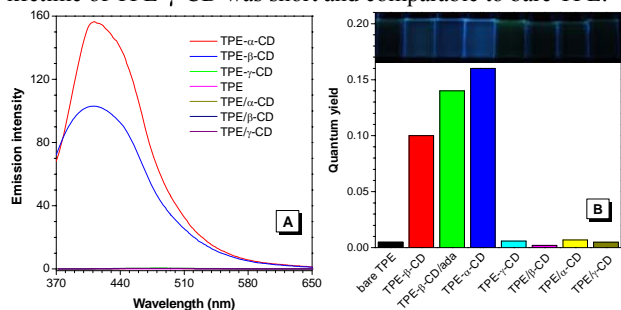


**Fig. 2** (A) Fluorescence spectra and (B) quantum yield of TPE-CDs, bare TPE and TPE/CD mixtures (1:1 molar ratio) in DMSO solutions. Inset in (B): fluorescent photos of TPE-CDs, bare TPE and TPE/CD mixtures (1:1 molar ratio) in DMSO solutions taken under UV irradiation. Concentration: 5 mM.

Taking the advantages of their high quantum yield and good biocompatibility inherited from TPE and CD,<sup>1,11</sup> we explored the application of the TPE-CDs in biological science. As depicted in Fig. 3, the cytoplasm of HeLa cells incubated with TPE- $\beta$ -CD emitted upon UV irradiation, revealing that TPE- $\beta$ -CD was able to penetrate the cell membrane and worked as a fluorescent visualizer for intracellular imaging.

In summary, we developed a new strategy to restrict the motions of AIE molecules through host-guest inclusion, leading to the formation of a catalogue of new molecular luminogens. The phenyl rings of TPE were included in the cavity of cyclodextrins, resulting in enhanced fluorescence due to the restriction of their motions. The quantum yield of the TPE-CDs increased with decreasing the cavity size of the cyclodextrin. The TPE-CDs were biocompatible and could be utilized to image the cytoplasm of living cells.

This work was partially supported by the National Basic Research Program of China (973 Program; 2013CB834701), the Research Grants Council of Hong Kong (HKUST2/CRF/10 and N\_HKUST620/11) and the University Grants Committee of Hong Kong (AoE/P-03/08). B.Z.T. thanks the support from Guangdong Innovative Research Team Program of China (201101C0105067115). G.D.L thanks the support from the Hong Kong Scholar Program (XJ2011047) and NSFC (21374136).

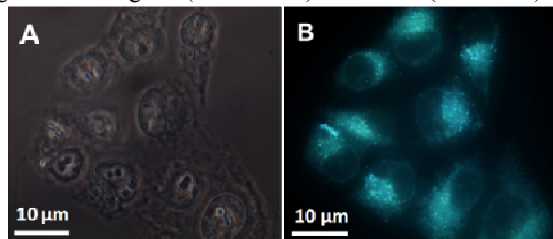


**Fig. 3** (A) Bright-field and (B) fluorescent images of HeLa cells incubated with TPE- $\beta$ -CD.

## Notes and references

- (a) Z. K. Wang, S. J. Chen, J. W. Y. Lam, W. Qin, R. T. K. Kwok, N. Xie, Q. L. Hu, B. Z. Tang, *J. Am. Chem. Soc.*, 2013, **135**, 8238–8245; (b) C. W. T. Leung, Y. N. Hong, S. J. Chen, E. G. Zhao, J. W. Y. Lam, B. Z. Tang, *J. Am. Chem. Soc.*, 2013, **135**, 62–65.
- (a) J. D. Luo, Z. L. Xie, J. W. Y. Lam, L. Cheng, H. Y. Chen, C. F. Qiu, H. S. Kwok, X. W. Zhan, Y. Q. Liu, D. B. Zhu, B. Z. Tang, *Chem. Commun.*, 2001, 1740–1741; (b) J. W. Chen, C. C. W. Law, J. W. Y. Lam, Y. P. Dong, S. M. F. Lo, I. D. Williams, D. B. Zhu, B. Z. Tang, *Chem. Mater.*, 2003, **15**, 1535–1546.
- Y. H. Xu, L. Chen, Z. Q. Guo, A. Nagai, D. L. Jiang, *J. Am. Chem. Soc.*, 2011, **133**, 17622–17625.
- J. Q. Shi, N. Chang, C. H. Li, J. Mei, C. M. Deng, X. L. Luo, Z. P. Liu, Z. S. Bo, Y. Q. Dong, B. Z. Tang, *Chem. Commun.*, 2012, **48**, 10675–10677.
- (a) S. N. B. hustova, B. D. McCarthy, M. Dinca, *J. Am. Chem. Soc.*, 2011, **133**, 20126–20129; (b) N. B. Shustova, T. C. Ong, A. F. Cozzolino, V. K. Michaelis, R. G. Griffin, M. Dinca, *J. Am. Chem. Soc.*, 2012, **134**, 15061–15070.
- (a) X. F. Ji, Y. Yao, J. Y. Li, X. Z. Yan, F. H. Huang, *J. Am. Chem. Soc.*, 2013, **135**, 74–77; (b) D. S. Guo, Y. Liu, *Chem. Soc. Rev.*, 2012, **41**, 5907–5921.
- (a) A. K. Mandal, M. Suresh, P. Das, A. Das, *Chem. Eur. J.*, 2012, **18**, 3906–3917; (b) R. Quintanilla-Licea, J. F. Colunga-Valladares, A. Caballero-Quintero, C. Rodriguez-Padilla, R. Tamez-Guerra, R. Gomez-Flores, N. Waksman, *Molecules*, 2002, **7**, 662–673; (c) H. F. riebolin, *Basic One- and Two-dimensional NMR Spectroscopy*, VCH Verlagsgesellschaft mbH: Weinheim, 1993, p275-281.
- (a) Y. M. Zhang, Z. X. Yang, Y. Chen, F. Ding, Y. Liu, *Crystal Growth & Design*, 2012, **12**, 1370–1377; (b) M. Miyachi, Y. Kawaguchi, A. Harada, *J. Incl. Phenom. Macro.*, 2004, **50**, 57–62; (c) M. Miyachi, A. Harada, *J. Am. Chem. Soc.*, 2004, **126**, 11418–11419.
- (a) A. Miyawaki, P. Kuad, Y. Takashima, H. Yamaguchi, A. Harada, *J. Am. Chem. Soc.*, 2008, **130**, 17062–17069; (b) Y. Liu, Z. L. Yu, Y. M. Zhang, D. S. Guo, Y. P. Liu, *J. Am. Chem. Soc.*, 2008, **130**, 10431–10439; (c) M. Paolino, F. Ennen, S. Lamponi, M. Cernescu, B. Voit, A. Cappelli, D. Appelhans, H. Komber, *Macromolecules*, 2013, **46**, 3215–3227; (d) Z. X. Zhang, K. L. Liu, J. Li, *Macromolecules*, 2011, **44**, 1182–1193.
- Y. Liu, A. J. Qin, X. J. Chen, X. Y. Shen, L. Tong, R. R. Hu, J. Z. Sun, B. Z. Tang, *Chem. Eur. J.*, 2011, **17**, 14736–14740.
- (a) Y. Ping, C. D. Liu, Z. X. Zhang, K. L. Liu, J. H. Chen, J. Li, *Biomaterials*, 2011, **32**, 8328–8341; (b) H. L. Huang, H. Yu, G. P. Tang, Q. Q. Wang, J. Li, *Biomaterials*, 2010, **31**, 1830–1838.